

# Asymmetries in young supernova remnants: the case of Tycho

Moranchel-Basurto A.<sup>1</sup>, Velázquez, P. F.<sup>1</sup>, Schneider, E. M.<sup>2,3</sup>, Esquivel A.<sup>1</sup>

<sup>1</sup>Instituto de Ciencias Nucleares, Universidad Nacional Autónoma de México, CP: 04510, Mexico City, México

<sup>2</sup>Instituto de Astronomía y Teórica y Experimental, CP: X5000BGR, Córdoba, Argentina

<sup>3</sup>Departamento de Materiales y Tecnología, Universidad Nacional de Córdoba, CP: X5016GCA, Córdoba, Argentina.



Abstract

We have developed three-dimensional MHD numerical simulations using the "Guacho" code, in order to explore the scenario in which the initial mass distribution of a Supernova (SN) explosion is anisotropic. The idea is to analyze if this scenario can explain the radio-continuum emission and the expansion observed in young supernova remnants (SNRs), such as the case of Tycho's SNR. From our numerical results, synthetic polarized synchrotron emission maps were computed. Also and based in these synthetic maps, an expansion study was carried out. We have found a good agreement of this expansion study with previous observational results applied to the Tycho's SNR. Additionally, both the observed morphology and the brightness distribution are well reproduced.

## 1 Introduction

Observations of Supernova Remnants (SNR) exhibit asymmetries in their morphologies and in their emission patterns (in radio and/or X-rays). For example the morphology of Tycho supernova remnant at radiofrequencies is not completely spherical. In fact, the western side of the shell is well defined, while the eastern side looks more evolved and expands at lower speed with respect to the western side [6].

Our goal is to model the radio continuum emission from the Tycho's SNR making 3D MHD simulations computed with the Guacho code. We employ the same scenario given by [11]. In that work they suggested that the asymmetry observed in X-ray images of Tycho's SNR can be explained by the impact of an SNR shock wave on the companion star. After the collision, the SNR shock sweeps up material from the upper atmosphere of the companion star, generating an asymmetric density distribution. The collision between the shock wave of an SN and its companion star has been studied numerically by [5]. They found that if the companion is a main-sequence star it can lose about 15% of its mass, while an RG companion can lose up to 98% of its envelope. Additionally we develop an expansion study with our numerical results and we compare our results with expansion study made by [6], based on high-resolution radio data obtained with the VLA (Very Large Array).

## 3 Results

### 3.1 Synchrotron emission: synthetic maps

We obtained the synthetic maps from our numerical simulation by employing the Stokes parameters in terms of the magnetic field Eqs.(1)-(4) [9].

$$I = 2F(p)\nu^{\frac{1-p}{2}} \int d\Omega \int dz (B_x^2 + B_y^2)^{\frac{p-3}{4}} (B_x^2 + B_y^2) \quad (1)$$

$$Q = -2G(p)\nu^{\frac{1-p}{2}} \int d\Omega \int dz (B_x^2 + B_y^2)^{\frac{p-3}{4}} (B_x^2 - B_y^2) \quad (2)$$

$$U = -2G(p)\nu^{\frac{1-p}{2}} \int d\Omega \int dz (B_x^2 + B_y^2)^{\frac{p-3}{4}} (B_x^2 B_y^2) \quad (3)$$

$$I_p = \sqrt{Q^2 + U^2}, \quad (4)$$

where  $\nu = \frac{c}{\lambda}$ ,  $\lambda$  is the observed wavelength,  $p$  the spectral index for the electron distribution and:

$$F(p) \propto C_2 v^{2(p-1)} \rho \frac{2^{\frac{p+1}{2}}}{p+1} \quad (5)$$

$$G(p) \propto C_2 v^{2(p-1)} \rho \frac{2^{\frac{p-3}{2}}}{2} \quad (6)$$

being  $v$  and  $\rho$  the velocity magnitude and the density of the gas, respectively, while  $C_2$  is a function which includes the dependence with the obliquity angle  $\theta_B$  (the angle between the normal shock and the magnetic field) which can be written as [8]:

$$C_2 \propto \cos^2 \theta_B + \frac{1}{1+\eta^2} \sin^2 \theta_B \quad (7)$$

In Eq.(7) both acceleration mechanism of the relativistic particle in the main SNR shock front are presented: the quasi-parallel one (proportional to  $\cos^2 \theta_B$ ) and quasi-perpendicular one (proportional to  $\sin^2 \theta_B$ ). The parameter  $\eta$  can be estimated by [8]:

$$\eta = \frac{B^2}{\langle \delta B^2 \rangle} \quad (8)$$

where  $B$  is the magnitude of the mean magnetic field and  $\delta B$  is the magnetic field perturbation. Eq.(8) shows the  $\eta$  parameter indicates if the magnetic field is ordered ( $\eta \geq 1$ ) or a not ( $\eta \ll 1$ ).

In order to estimate  $\eta$  we employ the limit value given by [12]:

$$\frac{\langle \delta B^2 \rangle}{4\pi} \approx \left( \frac{V_A}{V_s} \right)^{1/2} \rho V_s^2 \quad (9)$$

being  $1/2\rho V_s^2$  the upstream flow energy density in the shock frame,  $V_s$  the shock front velocity, and  $V_A$  the Alfvén velocity, which is given by:

$$V_A = \frac{B}{\sqrt{4\pi\rho}} \quad (10)$$

## 4 Conclusions

- Our work is based on the scenario of an asymmetrical explosion, proposed by [11] for modelling the thermal X-ray emission of this remnant. Our results shown that this scenario is also able to explain the morphology in radio of this object, and also reproduces the expansion rates reported by [6]. In other words, the same asymmetrical explosion scenario can reproduce the morphology of this object at two different frequencies.
- We obtained synthetic maps of the synchrotron emission considering mass excess of 0.3 and 0.6  $M_\odot$ . The magnetic field was orientated along to the y-axis. The better concordance with the Tycho morphology was obtained after applying a rotation  $(-90, 15, 0)$  with respect to the x-, y-, and z-axes respectively and considering the quasi-perpendicular acceleration mechanism. In our synthetic maps we observed a clear dependence of the synchrotron emission with respect to the gas velocity, since the zone 1 was initially with a lower mass.

## References

1. Bandiera R., Petruk O., 2016, MNRAS, 459, 178
2. Boechino F., Orlando S., Miceli M., Petruk O., 2011, A&A, 531, A129
3. Cecere M., Velázquez P. F., Araudo A. T., De Colle F., Esquivel A., Carrasco-Gonzalez C., Rodríguez L. F., 2016, ApJ, 816, 64.
4. Giacani E. B., Dubner G. M., Green A. J., Goss W. M., Gaensler B. M., 2000, AJ, 119, 281.
5. Marietta, E., Burrows, A., Fryxell, B. 2000, ApJ, 128, 615
6. Reynoso E. M., Moffett D. A., Goss W. M., Dubner G. M., Dickel J. R., Reynolds S. P., Giacani E. B., 1997, ApJ, 491, 816.
7. Reynoso E.M., Velázquez P.F., Dubner G.M. and Goss, W.M., 1999, Aj, 117, 1827.
8. Reynolds S.P., 1998, ApJ, 493, 375.
9. Petruk O., Bandiera R., Beshley V., Orlando S., Miceli M., 2017, MNRAS, 470, 1156.

## 2 Simulation Details

The numerical simulations were carried out with the 3D MHD code Guacho. We impose an asymmetrical mass distribution of the SN (see Figure 1) Additionally we have considered a uniform component associated with the Galactic magnetic field  $B$ . We follow the expansion of the remnant until an integration time of 450yr.

Parameter	Value
$B$	$5 \times 10^{-6}$ G
$E_{sn}$	$1 \times 10^{50}$ erg
$M_{sn(zone1)}$	$0.7 M_\odot$
$M_{sn(zone2)}$	$1.3 - 1.0 M_\odot$
$\rho_{ism}$	$0.25 \text{ cm}^{-3}$
$\xi$	0.90
$X_{max}$	9pc (800pixels)

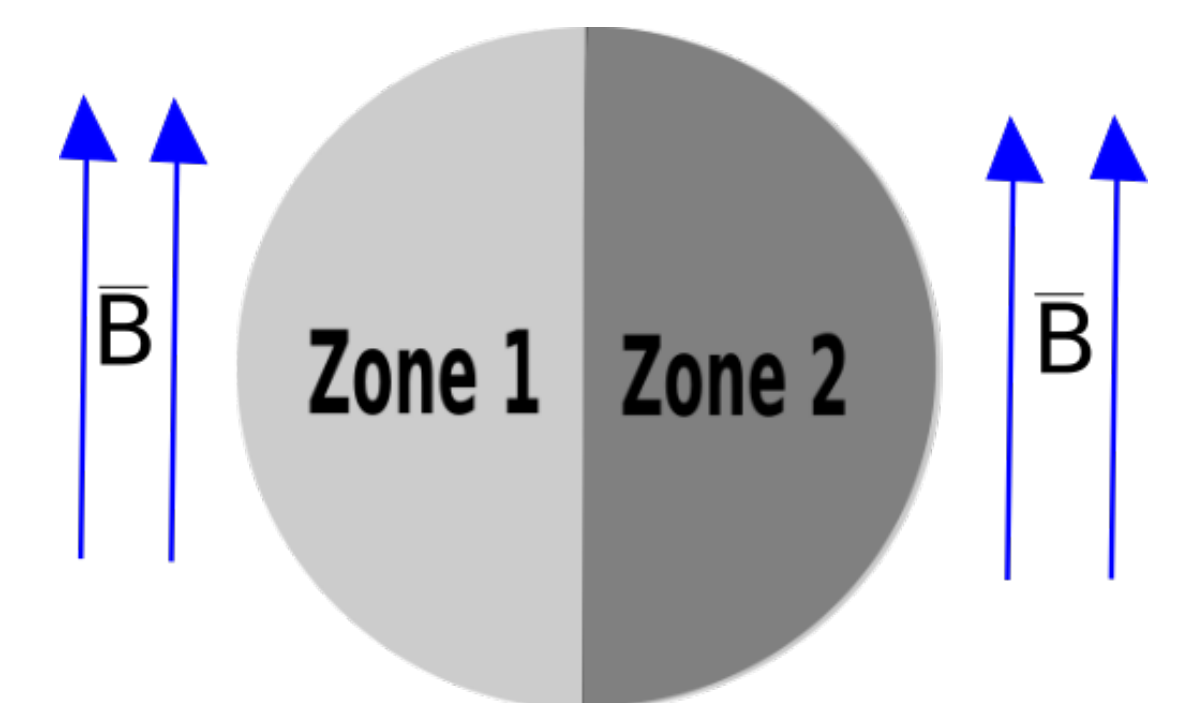


Figure 1: Scheme of the configuration employed in our simulations.

The ratio  $V_s/V_A$  is the Alfvénic Mach number of the shock  $M_A$ . Considering Eq.(9) and (10), we obtain  $\langle \delta B^2 \rangle / B^2 \approx V_s/V_A = M_A$ . Based on this, we can write Eq.(8) in the following way:

$$\eta = \frac{1}{f_{ef} M_A} \quad (11)$$

where we have introduced a free parameter  $f_{ef}$ , which can allow us to choose the acceleration mechanism (i.e.,  $f_{ef} \ll 1$  gives the quasi-parallel case, while  $f_{ef} \sim 1$  corresponds to the quasi-perpendicular case)

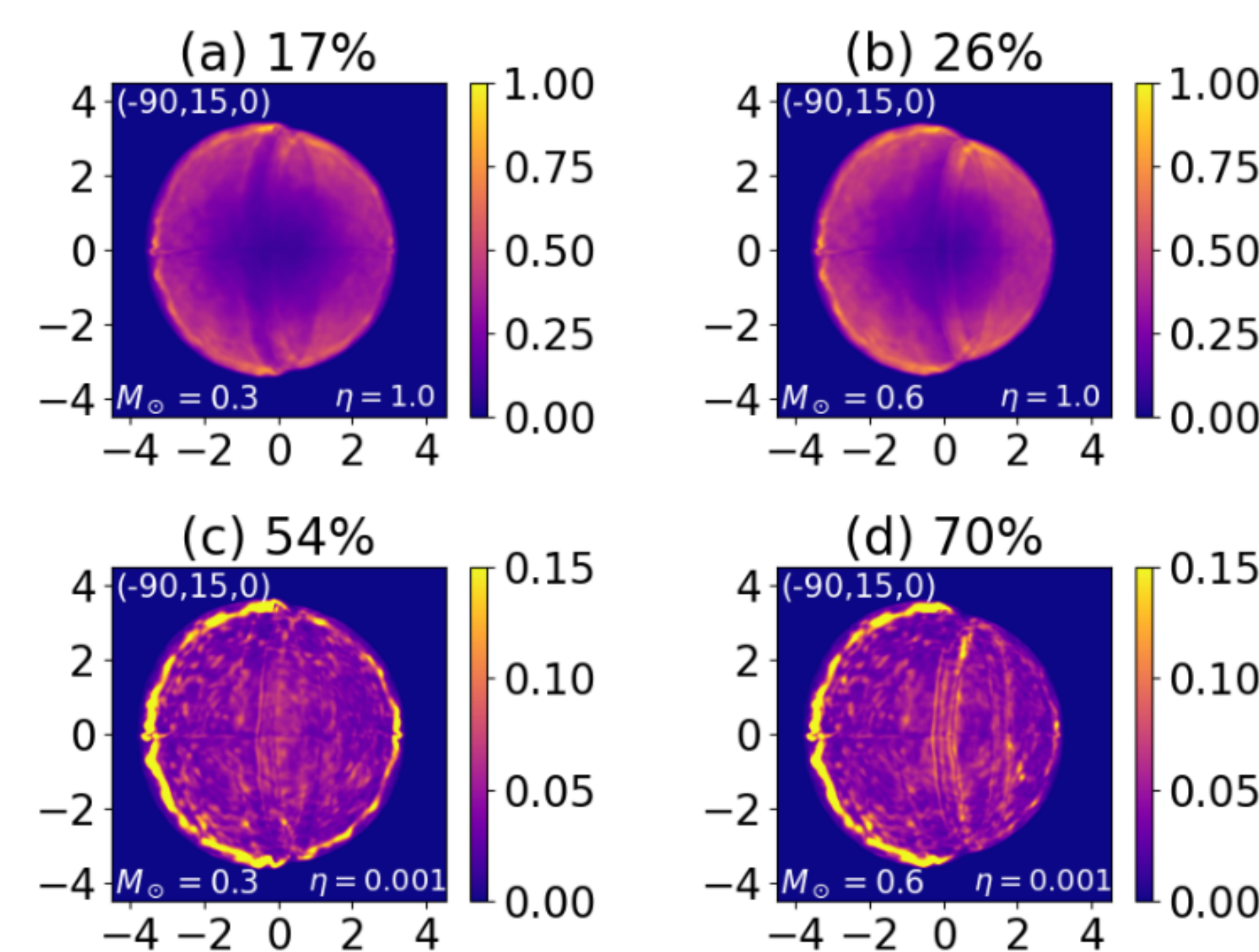


Figure 2: Comparison for the synchrotron emission maps between excess of mass of  $0.3M_\odot$  (plot (a) and plot (c)) and  $0.6 M_\odot$  (plot (b) and plot (d)). The plots (a) and (b) corresponds to the quasi-perpendicular case while the plots (c) and (d) corresponds to the quasi-parallel case. The percentage indicated in the upper part of each figure represents how bigger is the emission of the left part with respect to the right part. The axes are given in units of pc.

### 3.2 Expansion study

We performed runs over a 10 years intervals, since 400 to 460 years. Then we consider the radii at two successive times of our synthetic synchrotron emission maps, which will be called evolution 1 and evolution 2 (where evolution 2 is evolution 1 plus 10 years). We take account 18 azimuthal sections and for each one of these we found the corresponding expansion factor for by employing the equation (12) for both evolution frames as follow:

$$m = \frac{\log(R_2/R_1)}{\log(t_2/t_1)} \quad (12)$$

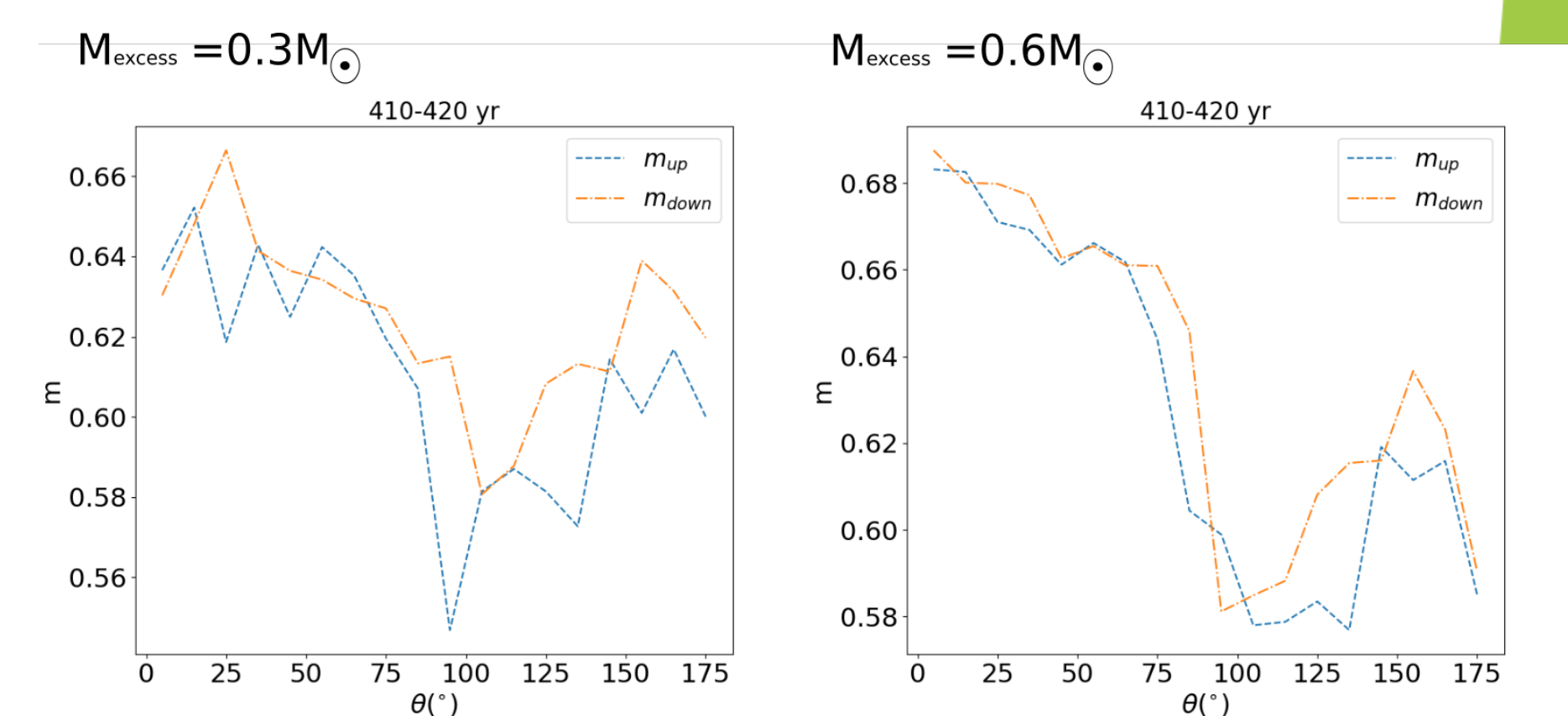


Figure 3: The graphics shown the values obtained for the expansion parameter at the time interval corresponding to 410-420 years for the cases of a mass excess of  $0.3M_\odot$  and  $0.6M_\odot$ .

Zone <sub>R</sub>	Zone	$m_R$	$m_{0.6}$	$m_{0.3}$
I				
(0° - 40°)	1	$0.497 \pm 0.006$	0.59	0.59
II				
(60° - 80°)	1	$0.246 \pm 0.006$	0.59	0.59
III				
(90° - 130°)	1	$0.57 \pm 0.01$	0.59	0.59
IV				
(140° - 180°)	1	$0.568 \pm 0.008$	0.59	0.59
V				
(200° - 345°)	2	$0.646 \pm 0.003$	0.66	0.63

Table 1: Comparison with observational values found for the Tycho remnant. The first and third columns are the results found by [6], while the second, four and five columns are our results. The first and second columns corresponding to different azimuthal regions while the third, fourth and fifth columns are the expansion parameter found by [6] and considering an excess of mass the 0.6 and  $0.3M_\odot$  respectively

We can see in the table 1 that the greatest discrepancy in the results corresponds to zone II of [6] with an expansion of 0.2, which is due to the fact that in this region the SNR shock wave is colliding with a dense clump, observed in HI [7]. However in the rest of the areas we find a good agreement in both observational and ours results.

10. Schneider E. M., Velázquez P. F., Reynoso E. M., Esquivel A., De Colle F., 2015, MNRAS, 449, 88.

11. Vigh C.D., Velázquez P.F., Gmez D.O., Reynoso E.M., Esquivel A., Matias Schneider E., 2011, ApJ, 727, 32.

12. Völk, H. J., Berezhko, E.G., Ksenofontov L.T. and Rowell G.P., 2002, AAP, 396, 649.

13. West J. L., Safi-Harb S., Jaffe T., Kothes R., Landecker T. L., Foster T., 2016, A&A, 587, A148

## Acknowledgements

AM-B, PFV, and AE, acknowledge financial support from DGAPA-PAPIIT (UNAM) grant IG100218. AM-B is a fellow CONACyT (México). EMS is member of the Carrera del Investigador Científico de CONICET, Argentina. We thank Enrique Palacios-Boneta (cómputo-ICN) for maintaining the Linux servers where our simulations were carried out.